Sustainable Energy, Grids and Networks 33 (2023) 100982

Contents lists available at ScienceDirect

Sustainable Energy, Grids and Networks

journal homepage: www.elsevier.com/locate/segan

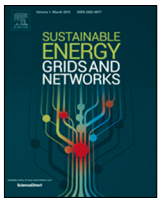

A stochastic approach for self-healing capability evaluation in active islanded AC/DC hybrid microgrids

Salar Moradi *, Gaetano Zizzo, Salvatore Favuzza, Fabio Massaro

Engineering Department, University of Palermo, Building 9, Palermo, Italy

ARTICLE INFO

Article history:
Received 18 February 2022
Received in revised form 26 September 2022
Accepted 11 December 2022
Available online 16 December 2022

Keywords:
Resilience
Self-healing
AC/DC hybrid microgrids
Flexible sources
Stochastic analysis
Optimal power flow
Monte-Carlo simulation

ABSTRACT

This paper aims to implement a resilience assessment in AC/DC hybrid microgrids using a stochastic simulation approach. Self-healing measures including load shedding, control of distributed generation and flexible devices, like Energy Storage Systems (ESS) and Electrical Vehicles (EVs), are simulated to enable AC/DC hybrid microgrids to supply critical loads in islanded mode, assuming a disconnection of these microgrids from the main AC grid due to a fault. To perform this analysis, a two-stage process is proposed: first, a Monte-Carlo simulation-based stochastic approach is adopted to generate samples to simulate intermittent loads, power generation from Renewable Energy Sources (RESs), and fault occurs in the upstream grid; second, for each sample indicating islanded mode, a grid-connected daily Optimal Power Flow (OPF) is formulated in Mixed-Integer Linear Programming (MILP) form based on minimizing operation cost to withdraw the State of the Charge (SoC) of stationery and traction batteries and electrical vehicles before microgrids may go to islanded mode. Finally, resilience of islanded microgrids are evaluated through some indices. In addition, different strategies are considered for modeling the behavior of both two types of electrical vehicles V1G and V2G. Simulations results show distributed generation and flexible devices might improve resilience in islanded microgrids, optimal daily planning in grid-connected mode could affect it adversely though, due to the low energy available of flexible devices at the islanding moment.

1. Introduction

In recent decades, international decarburization goals, infrastructure development, demand side management, socio-economic issues, and the advent of new technologies such as renewable-based energy sources, energy storage systems (ESSs) as well as electrical vehicles (EVs), have increased interests to rebuilt traditional power systems. Microgrids, which are self-controlled networks that can operate in both grid-connected and isolated modes, are a practical approach to handle this challenge [1,2].

Although the traditional AC power system has been the most developed system in the past few decades and many of our existing loads are of AC in nature, the appearance of power electronics and RESs with DC power generation, such as solar and fuel cells, has led to DC supply implementation in modern grids. Today, the modern appliances — laptops, mobiles, remote controllers, EVs, etc. are operating on DC supply that facilitates easy control without power factor, phase sequence, power angle and frequency issues [3]. Therefore, AC/DC hybrid smart grids can have advantages of both AC and DC networks including reliability improvement for less electronic elements and more power supply feeders (depending on topologies), power conversion loss reduction due to the decrease in ac–dc and dc–ac converters, simple control, more power transmission capacity, and economic benefits [4–7].

Challenges

With the advent of modern AC/DC hybrid microgrids, new challenges have arisen especially in term of sustainable power supply. Self-healing capability assessment is one of the most significant issues. In particular, it is fundamental to find out to what extent a smart hybrid microgrid in island mode is capable to provide customers with safe electrical energy in emergencies and in different energy scenarios. Self-healing capability is one of the main features of smart distribution systems and an effective way to increase the network reliability by having recourse to the control of flexible loads, renewable energy sources (RESs), energy storage systems and electrical vehicles in an emergency due to a fault causing the interruption of supply from the main grid. So, it appears to be critical to define some resilience indices for assessing the effects of the self-healing measures mentioned above. In this context, an important challenge is posed by the

* Corresponding author.
E-mail addresses: salar.moradi@community.unipa.it (S. Moradi), gaetano.zizzo@unipa.it (G. Zizzo), salvatore.favuzza@unipa.it (S. Favuzza), fabio.massaro@unipa.it (F. Massaro).

https://doi.org/10.1016/j.segan.2022.100982
2352-4677/

Table 1
Previous works comparison.

Ref. No.	Method	Advantages	Disadvantages
[8]	Nested restoration decision system (minimizing unused DGs output in microgrids)	• Apply to complex networked microgrids • Increase resilience in island mode • Facilitate frequency and voltage restoration in island mode	• Not consider intermittent nature of RESs and loads • Not apply to whole a day; so not analysis the effect of different consumption cases • Not consider RESs and EVs • Applicable only to AC grids
[9]	Stochastic rolling-horizon optimization to sectionalize	• Using dispatchable DGs and control them in islanded mode • Apply to networked microgrids • Self-healing assessment for multiple faults	• Not consider EVs • Applicable only to AC grids • Not evaluate how different DGs capacity may affect the goals.
[10]	Re-dispatch, load shedding and network reconfiguration using mixed-integer quadratic programming	• Apply to active multi microgrids enabling buying/selling energy from/to the main grid • To assess different generation and load scenarios	• Not consider intermittent nature of RESs and loads • Not consider RESs and EVs • Applicable only to AC grids
[11] [12]	Re-dispatch, load shedding and network reconfiguration using mixed-integer linear programming	• Multi-objective optimization • Comparison to different methods • Control of technical parameters like voltage and frequency	• Not consider RESs, ESS and EVs • Not consider intermittent nature of loads • Applicable only to AC grids
[13]	Re-dispatch, load shedding and network reconfiguration using daily optimal power flow	• Probabilistic generation and load model • Different control strategies	• Not consider EVs • Applicable only to AC grids
[14] [15]	Two-stage robust optimization	• Fast and reliable self-healing process • Cover comprehensive restoration process • To address uncertainty for wind generation • Voltage stability assessment	• Just consider wind farm and hydro pump storage system • Not evaluate uncertainty for load • Applicable only to AC grids
[16]	Two-layered metaheuristic algorithm for optimal formation and optimal DERs allocation	• Taking into account network constraint • Implement RESs and storage system • Load, fault and generation estimation	• Not to take into account EVs • Use flexible sources discharge only in off-grid mode • Applicable only to AC grids
[17] [18]		• To handle technical tasks like feeders' congestion, voltage violations, active and reactive power devices coordination • To analysis the importance of a communication protocol system	• Not consider RESs and flexible sources • Not address load and fault uncertainty • Not implement energy management
[19] [20]	Two-layered optimal power flow	• To control in both normal and self-healing modes • Application of multiple faults • Different energy scenario assessment	• Evaluating self-healing mode only for a few time slots • Not include EVs • Applicable only to AC grids
[21]	Four-layered agent-based control scheme	• Real-time monitoring • Dynamic performance assessment • Control scheme for all component	• Self-healing mode is evaluated only for a few hours • EVs are not included • Applicable only to AC grids

intermitted behavior of RESs generation, loads, and the changing state of charge (SoC) of ESSs and EVs which must be considered to obtain a more realistic result from the analysis.

Literature Review

For better understanding the importance of the present analysis, firstly it must be approached by analyzing the state of the art. In [8], authors try to implement a new networked microgrids formation which aims to minimize unused generation capacity in islanded mode through a nested restoration decision system. Energy exchange in this paper is based on a layered control strategy from outer layers to inner ones. In [9], a new self-healing and operation strategy analysis of distribution networks is performed using a stochastic rolling-horizon optimization in grid-connected mode to make an optimal decision for sectionalizing isolated sections into self-adequate microgrids. In [10–12], the authors present self-healing measures such as generation re-dispatch, load shedding and network reconfiguration. This problem is optimized and solved using mixed-integer quadratic/linear programming to obtain an optimal island switching. In [13], the authors propose an operational plan for performing an optimum self-healing actions including load shedding, system reconfiguration and Distributed Generation (DG) output control, considering self-adequacy, total energy losses, and total supplied loads based on their priority. Both planning and real-time phase's restoration as self-healing actions are combined into one optimization problem to respond to contingency situations in [22]. The works [14,15] propose self-healing capabilities by coordination strategy of wind and pumped-storage hydro units in restoration phase and speeding up the recovery process using partitioning islanded power grid and considering technical limits, respectively. A two-layer metaheuristic algorithm is proposed in [16] for the optimal operation of smart distribution networks in self-healing mode considering wind turbines and energy storage systems. In the first layer, a graph theory finds an optimal formation, while the second one aims to find the optimal energy management. The works [17,18] propose a Fuzzy multi-agent system applied in distribution networks to restore the maximum loads and minimize the number of switching time intervals. The works [19,20] implement a decentralized two-layer Energy Management System (EMS) for a networked microgrid which operates independently. In emergency analysis, EMSs in both layers make the optimal decision to supply the on-emergency microgrid through an average consensus algorithm and a bi-level stochastic optimization algorithm, respectively. A heuristic algorithm has been proposed in [23], which presents self-healing strategy to mitigate cyber-attacks. The work [21] employs a four-layer multiagent concept including different energy management and control strategies as self-healing capabilities to improve dynamic performance of microgrids. Finally, in [24,25] a simulation analysis is presented and some reliability indices are defined for three different hybrid AC/DC microgrids showing the behavior of the microgrids in islanded modes in different energy scenarios. Table 1 represents comparison between some of these works indicating their methods, advantages and disadvantages.

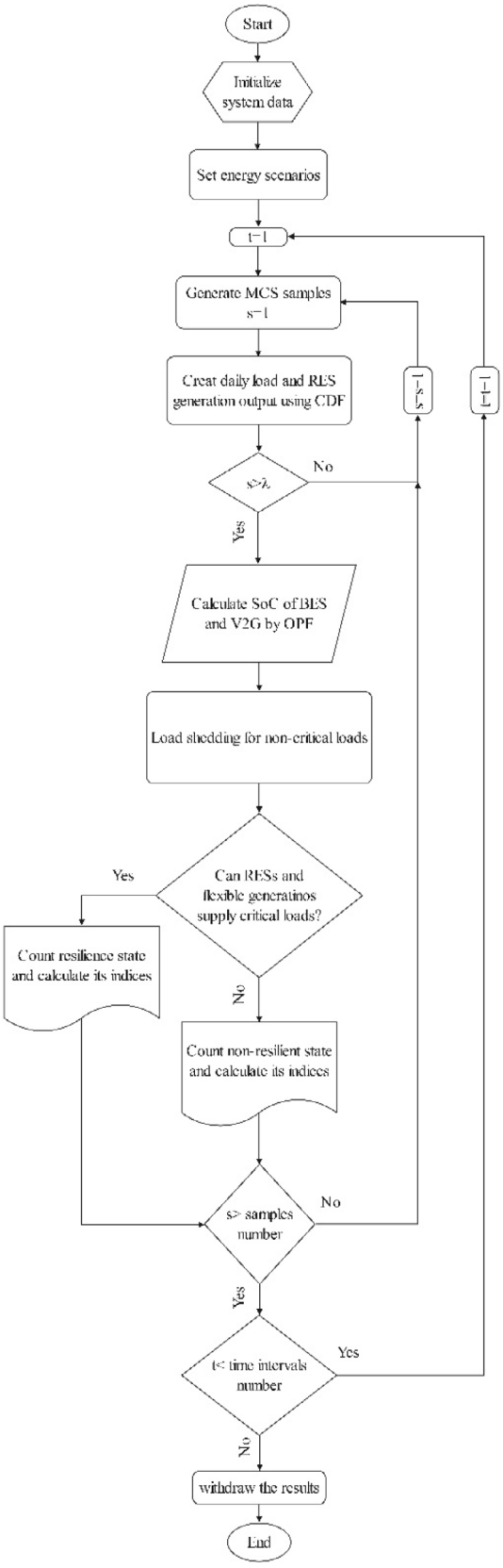

Fig. 1. Overall process of the proposed methodology.

Contributions

In this framework, according to Table 1, some research gaps are discussed that have been addressed in this work to show the importance of applying the proposed methodology. Firstly, previous works did not take into account AC/DC microgrids self-healing capability and the impact of various energy scenarios, whereas this work presents a methodology for performing a comprehensive self-healing assessment for AC/DC MV/LV hybrid microgrids considering the specific characteristics of the distributed flexible resources and the impact of the energy scenario. The methodology is applied to three microgrids: an underground station, a car park, and a residential area where five energy scenarios characterized by different energy consumption, RES production, number of EVs and controllable loads are defined for assessing the self-healing capability in presence of different shares of flexible devices. The diversity of the load profiles, of the entity of the critical loads and of the flexible resources considered in the study, contribute to the novelty of the research. The scenarios refer to the years 2022, 2030 and 2040 and have been defined according to the most recent technical reports on the energy transition in Europe and Italy [26–31].

In addition, an optimal power flow (OPF) using Mixed-Integer Linear Programming (MILP), considering the connection of the main AC upstream network and proper stochastic approaches for variable parameters, is carried out to determine the SoC of ESSs and EVs before an interruption of the main MV AC grid due to a fault event by which we can recognize how optimal energy management in normal condition may affect self-healing in off-grid mode; however, other works do not calculate the SoC of flexible sources in an microgrids in this paper are fully-equipped with all RESs and flexible sources, especially EVs that not taken account in above-mentioned works.

It is assumed that the microgrids can operate independently in islanded mode supplying with their local resources the critical loads. Furthermore, a Monte-Carlo simulation is implemented to calculate a set of resilience indices representing the capability of the islanded hybrid microgrids of supporting customer's power supply in the different energy scenarios. These indices can be categorized into customer- energy- and microgrid-oriented groups.

In brief, the main contributions of this paper can be resumed as it follows:

- proposing a study that considers different energy scenarios for assessing the impact of the increase in the flexible energy resources on the self-healing capability;
- calculation of the SoC of ESSs and EVs as flexible units through a pre-fault daily OPF with MILP formulation, and non-critical load shedding in self-healing mode;
- defining different valuable resilience indices to show to what extent microgrids are capable of providing a reliable supply to their critical loads;
- Implementing a stochastic approach to handle intermitted nature of variables such as load and renewable energy output, and Monte-Carlo simulation to calculate the set of resilience indices.

The remainder of this paper is organized as it follows: Section 2 contains a detailed description of the proposed methodology; Section 3 describes the AC/DC hybrid microgrids and the mathematical models of their elements such as loads, PV systems and EVs; Section 4 reports and discuss the results of the simulations; and, finally, Section 5 contains the concluding remarks.

2. Methodology

The methodology implemented in this paper is to assess self-healing in hybrid AC/DC microgrids consists of the steps depicted in Fig. 1.

In general, the steps in Fig. 1 can be grouped to distinguish two separate stages of the proposed methodology.

In the first stage, a failure is assumed to occur in the main AC grid, which is simulated through random value samples called Mont-Carlo samples. Comparing the random samples to the rate of microgrid (failure rate of AC main grid [32]), island and grid-connected modes can be found out, so that if random value is less than the failure rate, it is assumed there is an islanded mode and failure in the main grid has accrued, and if it is greater than the failure rate, network operates in normal or grid-connected mode. Referring to the database from ARERA, the Italian Regulatory Authority for Energy, Networks and the Environment, the average duration of the fault is assumed 45 min for MV and LV AC distribution grids [33].

It is worth underlying that, the installed local generating capacity of each microgrid is not enough to supply all loads; therefore, when a microgrid is in islanded mode due to a failure of the main grid, the non-critical loads with high consumption are disconnected. Since the aim of this study is to evaluate the capability of hybrid microgrids of supplying critical loads during off-grid operation through RESs, load shedding, and flexible generations such as ESS and smart EVs, it is significant to identify the operation state of these resources.

Renewable energy sources' power output is completely independent from the operation modes of the network, since it depends on environment conditions, such as wind speed or solar irradiation. Flexible resources charging/discharging states, instead, vary according to the consumption and operation mode (grid-connected or islanding) of the microgrid. Therefore, the SoC of ESSs and EVs must be calculated before the fault event occurs in the main grid. For performing this calculation, an OPF-based energy management is implemented. The OPF is formulated based on minimizing the operation cost for each time interval and random sample. There are several works addressing stochastic energy management in microgrids that one comprehensive is [34] which here simpler version is used. So, the objective function for each microgrid is:

$$C_{op} = \sum_{t} c_g P_g(s,t) \qquad \forall e, m, s \tag{1}$$

All symbols explanation is reported in Appendix.

Equations and inequalities (2)–(4) represent generation-related constraints. Eq. (2) is the daily power balance for a generic microgrid; Eqs. (3) and (4) represent the output power limit for PV and wind generators. Because the installed capacity of RES-base generators is constant and this paper projects to analysis resilience in off-grid mode, power purchased from the AC main grid in not restricted to its limit, meaning, in grid-connected mode, microgrids' loads are surely going to be supplied, so there is no restriction in power importing from the main grid.

$$P_g(s,t) + P_{pv}(s,t) + P_w(s,t) + P_s^{dis}(s,t) + P_{v2}^{dis}(s,t) = P_l(s,t) + P_s^{ch}(s,t) + P_{v2}^{ch}(s,t) \qquad \forall s, t, m, e \tag{2}$$

$$P_{pv}(s,t) \le \eta P_{pv}^{\max}(m) \qquad \forall s, t, m, e \tag{3}$$

$$P_w(s,t) \le \eta P_w^{\max}(m) \qquad \forall s, t, m, e \tag{4}$$

Constraints (5)–(11) express ESS's operation limits. Inequalities (5) and (6) indicate that charge and discharge powers of the EES must not exceed their bounds, and (7) expresses the non-simultaneity of battery charging and discharging operations. Eqs. (8) and (9) express the hourly available energy of the ESS, while (10) restricts this energy to its upper and lower limits. Furthermore, Eq. (11) is introduced to ensure that the energy stored at the end of a day is equal to the energy available at the beginning of the same day.

$$I_s^{ch}(s,t)P_{ch,s}^{\min} \le P_s^{ch}(s,t) \le I_s^{ch}(s,t)P_{ch,s}^{\max} \qquad \forall s, t, m, e \tag{5}$$

$$I_s^{dis}(s,t)P_{dis,s}^{\min} \le P_s^{dis}(s,t) \le I_s^{dis}(s,t)P_{dis,s}^{\max} \qquad \forall s, t, m, e \tag{6}$$

$$I_s^{ch}(s,t) + I_s^{dis}(s,t) \le 1 \qquad \forall s, t, m, e \tag{7}$$

$$E_s(s,t) = E_s(s,t-1) + P_s^{ch}(s,t) - P_s^{dis}(s,t) \qquad \forall s, t > 1, m, e \tag{8}$$

$$E_s(s,t) = U_s(0) + P_s^{ch}(s,t) - P_s^{dis}(s,t) \qquad \forall s, t < 2, m, e \tag{9}$$

$$E_s^{\min}(m) \le E_s(s,t) \le E_s^{\max}(m) \qquad \forall s, t, m, e \tag{10}$$

$$U_s(0) - \Delta U_s \le E_s(s,t) \le U_s(0) + \Delta U_s \qquad \forall s, t > 23, m, e \tag{11}$$

The following equations represent the constraints for EVs. They are formulated only for V2G EVs because they are the only EVs that can be managed by the network operator with an intelligent charge/discharge strategy. It means the SoC of V2G is variable unlike V1G whose charging is imposed as an input of the problem. Eqs. (12)–(18) have the same definition as those for ESS above. When V2G EVs are out of the zone, there is no charge and discharge operation for their batteries, which is expressed by (19) and (20). Finally, Eq. (21) implies that V2G must have a minimum energy at their battery when they leave the parking lot.

$$I_{v2}^{ch}(s,t)P_{ch,v2}^{\min} \le P_{v2}^{ch}(s,t) \le I_{v2}^{ch}(s,t)P_{ch,v2}^{\max} \qquad \forall s, t, m, e \tag{12}$$

$$I_{v2}^{dis}(s,t)P_{dis,v2}^{\min} \le P_{v2}^{dis}(s,t) \le I_{v2}^{dis}(s,t)P_{dis,v2}^{\max} \qquad \forall s, t, m, e \tag{13}$$

$$I_{v2}^{ch}(s,t) + I_{v2}^{dis}(s,t) \le 1 \qquad \forall s, t, m, e \tag{14}$$

$$E_{v2}(s,t) = E_{v2}(s,t-1) + P_{v2}^{ch}(s,t) - P_{v2}^{dis}(s,t) \qquad \forall s, t > 1, m, e \tag{15}$$

$$E_{v2}(s,t) = U_{v2}(0) + P_{v2}^{ch}(s,t) - P_{v2}^{dis}(s,t) \qquad \forall s, t < 2, m, e \tag{16}$$

$$E_{v2}^{\min}(m) \le E_{v2}(s,t) \le E_{v2}^{\max}(m) \qquad \forall s, t, m, e \tag{17}$$

$$U_{v2}(0) - \Delta U_{v2} \le E_{v2}(s,t) \le U_{v2}(0) + \Delta U_{v2} \qquad \forall s, t > 23, m, e \tag{18}$$

$$P_{v2}^{ch}(s,t) = 0 \qquad \forall s, q, m, e \tag{19}$$

$$P_{v2}^{dis}(s,t) = 0 \qquad \forall s, q, m, e \tag{20}$$

$$E_{v2}(s,t) \ge N\lambda D \qquad \forall s, T_l, m, e \tag{21}$$

In this paper a mixed-integer linear programming (MILP) formulation is considered to solve 24-hourly optimal power flow in GAMS/Cplex tool. GAMS/Cplex is a GAMS solver that allows users to combine the high level modeling capabilities of GAMS with the power of Cplex optimizers. Cplex optimizers are designed to solve large, difficult problems quickly and with minimal user intervention [35]. In the OPF problem with the contribution of flexible sources, there are integer variables such as charge/discharge of these units which cannot be done simultaneously. Therefore, mixed-integer solver is implemented to address this dilemma.

In islanded mode, since time horizon of self-healing in this paper is 15-min samples and not real-time, some significant parameters like voltage and frequency which have considerably effect on the load shedding could not be evaluated. In fact, it is assumed that these parameters, in island mode, would be fully controlled and there is not load shedding due to the voltage and frequency deviation. So, this paper only analyzes the microgrid self-healing capability of providing power supply to the critical loads.

In the second stage of the methodology, the SoC of ESSs and smart EVs calculated from the first stage is referred as input for the resilience assessment. A stochastic Monte-Carlo simulation generates random samples to distinguish grid-connected and islanded modes. In off-grid mode, it is proposed to find out whether available generation can supply critical loads or not. To evaluate this aspect, in island mode, it is necessary to evaluate some indicators, distinguishing between two sets. The first set consists of factors showing the resilience rate of microgrids, formulated as follows:

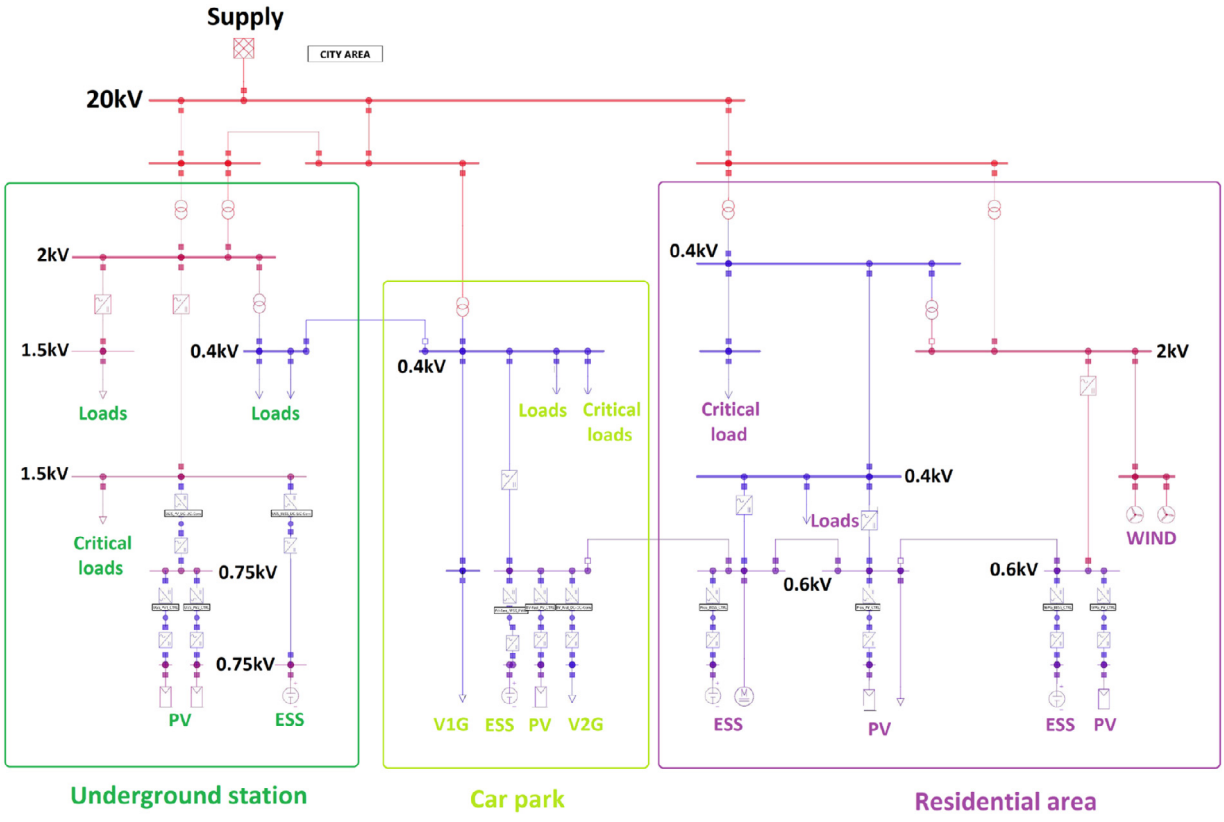

Fig. 2. City area network.

- The Resilience Frequency Rate (RFR) factor indicates how flexible microgrids are in supplying critical loads in island mode in a year:

$$RFR = \frac{\text{total number of resilient samples}}{\text{total number of islanding samples}} \tag{22}$$

- The Loss of Load Expectation ($LOLE$) index shows the number of days in which microgrids are not capable to provide enough power to supply critical loads in a year in islanded mode in a microgrid:

$$LOLE = (1 - RFR).365 \tag{23}$$

- The Resilience Duration Rate (RDR) represents the rate between the time T_r the microgrids are able to self-heal in islanded mode and the failure time in a year T_f:

$$RDR = \frac{T_r}{T_f} \tag{24}$$

The second set includes energy-oriented factors that imply generation status of RESs and flexible sources comparing to the energy consumed by the critical loads. These factors are defined below:

- The Renewable Energy Rate (RER) index shows the percentage of renewable sources energy available E^i_{RES} compared to the total energy consumed by critical load in a year E^c_l in islanded mode in a microgrid:

$$RER = \frac{E^i_{RES}}{E^c_l} \tag{25}$$

- The Flexible Energy Rate (FER) index shows the percentage of energy from flexible sources like EVs and ESSs E^i_F compared to the total energy consumed by critical load in a year E^c_l in islanded mode in a microgrid:

$$FER = \frac{E^i_F}{E^c_l} \tag{26}$$

- Energy not Supplied (ENS) factor which calculates the amount of energy not supplied by RESs and flexible resources in non-resilient cases during a year:

$$ENS = \sum_i (1 - RDR) P^c_l \tag{27}$$

3. Application to a hybrid AC/DC microgrids

Fig. 2. shows a MV/LV hybrid AC/DC distribution network defined for resilience studies like those presented in [24,25] and called "city area network". This network is supplied by a MV 20 kV AC upstream network through transformers. AC/DC converters are installed to support DC loads power and connect photovoltaic systems and ESSs to the DC buses. As it is clear from Fig. 2, three zones can be identified within the city area network: an underground station, a car park and a residential area, which can be operated as three independent microgrids when they are isolated from the main grid.

The underground station includes a DC system to provide electrical energy to the traction system and its relative services like lighting, air conditioning, commercial loads, etc. furthermore, there is a 400 V AC bus to supply surface station services. The car park microgrid comprises two buses: an AC bus supplying road services such as security point, video surveillance, lighting, etc, and a DC bus connecting PV, ESS, slow and fast EVs charging stations. As regards the residential zone, a 400 kVA substation provides power to the customers and there is a DC node connecting PV, ESS, and DC load [32]. Finally, in the same zone, a wind park provides energy to the loads.

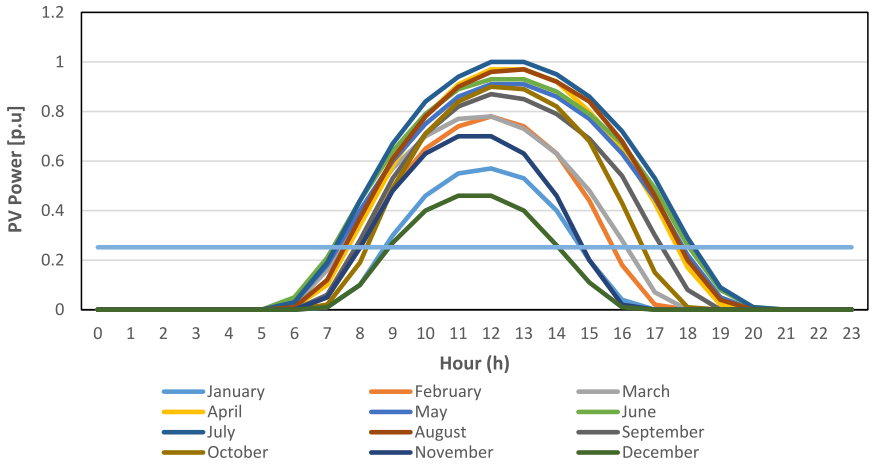

Fig. 3. Daily PV generation at LV network.

When a fault at the AC main grid occurs, if permanent, microgrids switch to off-grid operation and maintain it until service is restored or until local resources are able to supply critical loads. Assuming microgrid operators control the technical parameters like voltage and frequency, microgrids could be able to continue supplying loads through RESs, flexible resources like ESS and EVs, and load shedding. Therefore, these elements are modeled as follows to implement a simulation-based analysis.

3.1. Load

Daily consumption is one of the most significant uncertain variables in distribution systems. Therefore, it is vital for microgrid operators to manage this challenge in order to achieve a more realistic analysis. Probability analysis is a practical technique for obtaining a reliable estimate of these variables. According to the studies in the literature and looking at the trend of the daily consumption of the loads in the LV microgrids in Fig. 2, a normal Probability Density Function (PDF) is the best choice to refer to load uncertainty. The PDF for the load is expressed as follows:

$$N_m(l) = \frac{1}{\sigma\sqrt{2\pi}} \exp\left[-\frac{(l-\mu)^2}{2\sigma^2}\right] \tag{28}$$

where the mean of the load (μ) and the standard deviation (σ) can be extracted from the historical data reported in [32]. The above function is used for a Monte-Carlo simulation: it is assumed to generate a random probability number indication Cumulative Distribution Function (CDF) and return load variable at any given time using CDF inverse function.

3.2. Renewable energy sources

Photovoltaic and wind generation are other important elements which need to be modeled. In order to incorporate the RESs behavior in the microgrids' analysis, data regarding wind speed and solar irradiation are needed. Different PDFs for these types of variables have been proposed, anyway, Weibull and normal probability density function are used in this paper for the wind speed and PV power output, respectively, as follows:

$$W(w) = \frac{\beta w^{\beta-1}}{\alpha^{\beta}} \exp\left[-(\frac{w}{\alpha})^{\beta}\right] \tag{29}$$

$$N_m(P_{pv}) = \frac{1}{\sigma\sqrt{2\pi}} \exp\left[-\frac{(P_{pv}-\mu)^2}{2\sigma^2}\right] \tag{30}$$

Then, for any given wind speed which is calculated from the same Monte-Carlo simulation mentioned for the load above, the corresponding wind power output can be calculated as [36]:

$$P_w = \begin{cases} 0 & \text{for } w < w_i \text{ and } w > w_o \\ P_w^r(\frac{w-w_i}{w_r-w_i}) & \text{for } w_i \le w \le w_r \\ P_w^r & \text{for } w_r \le w \le w_o \end{cases} \tag{31}$$

Fig. 3 shows the normalized daily PV generation for each month of a year assumed in the present study, which proves why normal PDF matches PV power output.

3.3. Electrical vehicles

EVs are playing an important role in demand side management issue. They are considered as flexible load and resources which can be supplied during normal operation mode, or can compensate power shortage for critical loads during islanded operation mode. In this study, two types of EVs with different charge/discharge characteristics are considered:

- V1G EVs with dump charging strategy in which vehicles owners are completely free to connect and charge their vehicles whenever they want. The charging starts automatically when an EV plugs-in. Fig. 4 shows a daily average V1G EVs consumption for different seasons in the car park microgrid;
- V2G EVs with smart charging strategy. When this strategy is adopted, owners have to accept a commitment at which they share EVs' battery when the network needs this resource at both on-grid and islanded operation modes in technical and economical perspectives.

3.4. Energy scenarios

As explained in the introduction, the microgrid is studied considering different energy scenarios since it is interesting to assess to what extent the increase in RES production, available flexible resources such as controllable loads, ESSs and smart EVs is able to influence the self-healing capacity of the network.

The energy scenarios have been defined by analyzing the most recent technical report on the European and Italian energy transition [26–31] and are synthesized in Table 2. The data in Table 2 are reported in p.u. So that they can be adapted to the characteristics of any microgrid. In fact, it is not so much the absolute values of the quantities involved that characterize a scenario

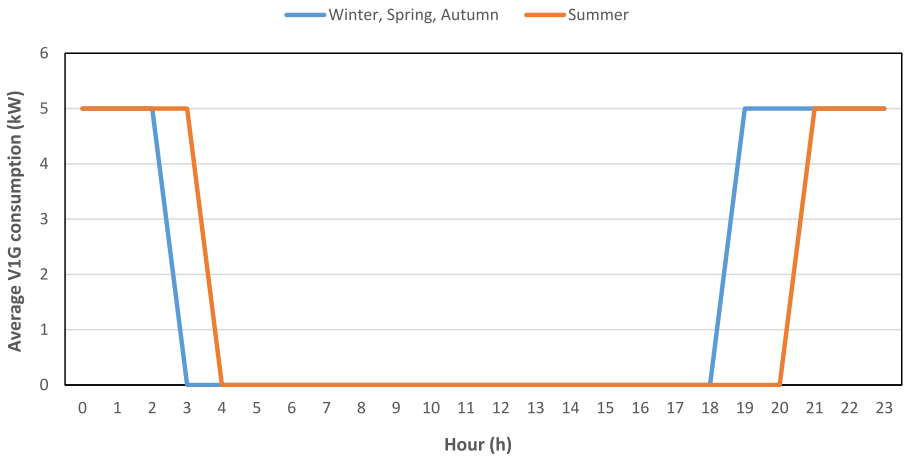

Fig. 4. Daily V1G consumption in car park area.

Table 2
Energy scenarios.

	2020	2030 BC	2030 DEC	2040 BC	2040 DEC
Final energy consumption	1 p.u.	1.08 p.u.	1.14 p.u.	1.16 p.u.	1.26 p.u.
Energy production from RES with respect to the total energy consumption	0.178 p.u.	0.212 p.u.	0.283 p.u.	0.287 p.u.	0.369 p.u.
Total RES generators rated power with respect of the total load power	0.47 p.u.	0.56 p.u.	0.70 p.u.	0.70 p.u.	0.83 p.u.
Total stationary EES rated power with respect of the total load power	8.7e−4 p.u.	1.23e−2 p.u.	1.16e−2 p.u.	8.70e−2 p.u.	8.10e−2 p.u.
Stationary storage capacity with respect to the load	1e−6 p.u.	1.12e−5 p.u.	1.07e−5 p.u.	8.03e−5 p.u.	7.42e−5 p.u.
Number of EVs	1 p.u.	83 p.u.	180 p.u.	180 p.u.	233 p.u.
Number of users participating in demand response programs	1 p.u.	1.000 p.u.	1000 p.u.	2500 p.u.	2500 p.u.

Table 3
City area energy scenarios.

	Energy scenarios for underground microgrid				
	2020	2030 BC	2030 DEC	2040 BC	2040 DEC
Daily energy consumption [kWh]	3694	3694	3694	3694	3694
PV systems rated power [kW]	109	130	170	175	175
ESS maximum capacity [kWh]	500	500	500	500	500
	Energy scenarios for car park microgrid				
	2020	2030 BC	2030 DEC	2040 BC	2040 DEC
Daily energy consumption [kWh]	653.5	973.5	973.5	1993	1993
PV systems rated power [kW]	20	35	45	90	120
ESS maximum capacity [kWh]	50	50	50	50	50
V1G EV [n]	5	10	10	25	25
V2G EV [n]	5	10	10	25	25
	Energy scenarios for residential area microgrid				
	2020	2030 BC	2030 DEC	2040 BC	2040 DEC
Daily energy consumption [kWh]	3696	3991.68	4213.44	4287.36	4656.96
PV systems rated power [kW]	33	43	60	62	87
Wind system rated power [kW]	33	43	60	62	87
ESS maximum capacity [kWh]	540	600	580	580	620

as the ratios between the sizes of the flexible resources and the energy/power requirements of each specific microgrid. Scenario 2020 is the base scenario representing the current situation, while scenario 2030 and 2040 represents the energy scenario in the next two decades. The suffixes BC and DEC indicates two different possibilities considered for the Italian energy transaction in the PNIEC (Italian Plan for Energy and Climate [37]). In particular, BC indicates the scenario Business-as-Usual, which inertially projects current trends and is characterized by technological development based on economic merit alone, and DEC indicates the scenario Decentralized, which achieves the decarburization, RES share and energy efficiency targets and the non-binding long-term CO_2 emission targets using a logic of minimizing decarburization costs and alternative technological developments. In the following, defined the rated power of the generators, the load power, the energy consumption and the characteristics of the flexible resources for the Scenario 2020 and for each microgrid, automatically, applying the coefficient in Table 2, the same data for the other scenarios will be defined.

4. Numerical results

In the simulations, it is assumed the failure rate of the MV network is 0.48 per year. All data for simulating total and critical load, electrical vehicles and battery energy storage system characteristics, PV and wind generation are taken from [32,33]. Referring these data, V2G vehicles with smart charge/discharge strategy leave the parking lot at 7 a.m. and arrive there at 7 p.m., with a 40 km average journey a day. V1G EVs are considered detachable load during off-grid operation. Table 3, shows the load, RESs and flexible resources data for the various energy scenarios in the three microgrids, calculated according to Table 2. In

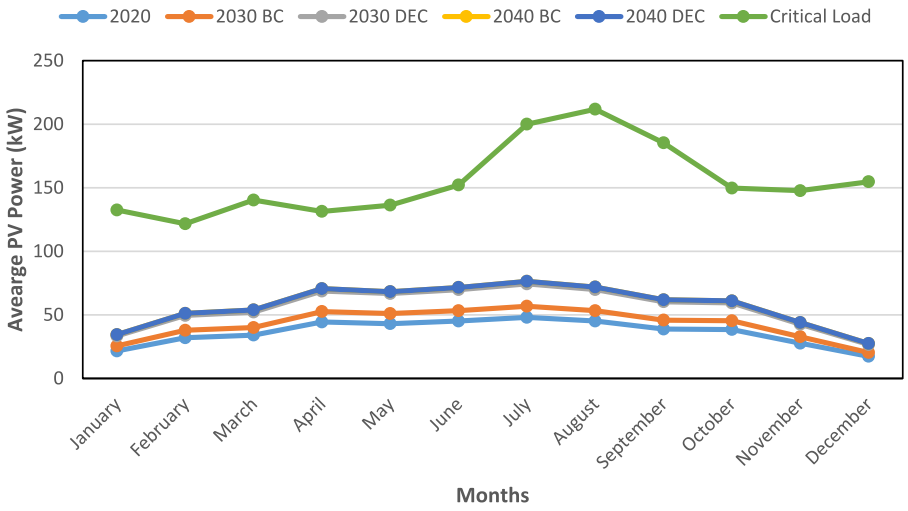

Fig. 5. Average available PV generation and critical load in islanded mode in the underground station microgrid.

Table 4
Resilience indices for underground area.

Underground area						
Scenarios	*RFR*	*LOLE* [day]	*RDR*	*RER*	*FER*	*ENS* [GW]
2020	0.59	149.1	0.65	0.2	0.23	7.6
2030 BC	0.74	93.6	0.79	0.24	0.36	2.6
2030 DEC	0.8	70.3	0.84	0.31	0.46	1.19
2040 BC	0.86	50	0.88	0.31	0.48	0.6
2040 DEC	0.86	50	0.88	0.31	0.48	0.6

Table 5
Resilience indices for car park area.

Car park area						
Scenarios	*RFR*	*LOLE* [day]	*RDR*	*RER*	*FER*	*ENS* [GW]
2020	0.5	183.6	0.62	0.43	0.5	0.5
2030 BC	0.66	122.5	0.8	0.68	0.47	0.1
2030 DEC	0.56	158.9	0.77	0.9	0.25	0.12
2040 BC	0.81	66.3	0.92	1.4	0.36	0.05
2040 DEC	0.92	22.3	0.97	1.9	0.32	0.01

Table 6
Resilience indices for residential area.

Residential area						
Scenarios	*RFR*	*LOLE* [day]	*RDR*	*RER*	*FER*	*ENS* [GW]
2020	0.9	36	0.93	0.11	0.47	0.13
2030 BC	0.82	64.5	0.87	0.14	0.42	0.78
2030 DEC	0.87	44.7	0.91	0.18	0.42	0.27
2040 BC	0.82	63.2	0.87	0.18	0.4	0.8
2040 DEC	0.65	127.5	0.72	0.25	0.33	3.9

the stochastic Monte-Carlo simulation 1000 random samples are considered. Since the islanding mode takes 45 min, time horizon is 15-min intervals in the OPF simulation. Therefore, there are 1000 × 96 samples in the proposed Mont-Carlo simulation.

Tables 4 to 6 report the indices defined in Section 2 and calculated for the various energy scenarios and for the three microgrids.

According to the data in Table 4, in the underground area it can be observed that a 37% increase in the installed PV power from the 2020 to the 2040DEC scenario results in an increase in *RFR* and *RDR* of 33% and 26%, respectively, indicating an increase in the self-healing capacity of the microgrid due to more availability of local generation from RESs in islanded mode. For the same reason the Loss of Load Expectation (*LOLE*) and the Energy not Supplied (*ENS*) indices decrease considerably in off-grid mode.

Figs. 5 and 6 show the average available PV power output, the critical load, and the average ESS energy for each month for the operation of the underground microgrid in islanded mode. A significant note here is the sharp drop in ESSs available energy in the summer months. As the load increases in the three summer months, and in all scenarios the PV power is less than the critical load in both on- and off-grid modes (Fig. 5), the OPF algorithm optimally determines the contribution of the ESS to supply the critical load. In fact, Eq. (6) implies that it is necessary to have a greater contribution from the ESS (Fig. 6) in the energy balance in order to purchase less energy from the main grid, resulting in lower operating costs. This situation is more evident in scenarios with low PV capacity and where the PV systems may not provide enough energy to charge the ESS in grid-on mode. On the other hand, the OPF causes the ESS to be fully discharged in daily operation. Therefore, during a failure (islanded mode), the average amount of energy of the ESS is not significant in July, August and September for 2020 and in August for 2030 BC.

Looking at Fig. 7, it can be seen that in the car park microgrid the average PV energy production available for the 2020, 2030 BC and 2030 DEC scenarios is just below the average critical load, while in both 2040 scenarios PV energy production far exceeds this load. Therefore, it is obvious that the increase in PV power leads to an increase in the island resilience of this microgrid, which results in an increase in the RFR, RDR, and in a drop in LOLE and ENS indices, so that, in the 2040 DEC scenario, we are faced with a highly resilient microgrid in which the RFR index takes on a value of 92%, as is shown in Table 5. Ultimately, since there is a significant difference between the available PV generation and the critical load in the last scenarios, this system can charge the ESSs and V2G EVs. Figs. 8 and 9 show the average available energy in isolated mode for all seasons.

These figures imply that, in first two scenarios with lower PV capacity, flexible resources do not contribute in daily OPF, because it is not optimal to charge these resources frequently during a day. Consequently, their average available energy in islanded mode is quite high. Whereas, in the 2030 DEC, 2040 BC, and 2040 DEC scenarios, the figures show a greater fluctuation in the available energy of flexible resources in isolated mode. In the 2030 DEC scenario, the OPF algorithm uses a lot of this energy to minimize operating costs, so that in the three months of April, August and October there is no energy available in island operation. Thus, this case is the worst from the resilience point of view (Table 5). For both 2040 scenarios, higher values of the available energy and thus of the SoC of the flexible resource batteries can

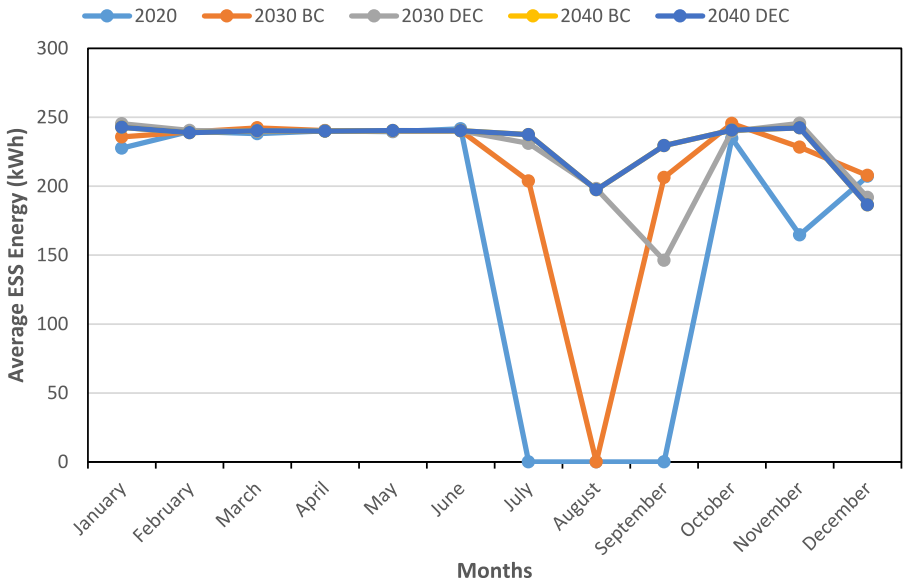

Fig. 6. Average available energy from ESS in islanded mode in the underground station microgrid.

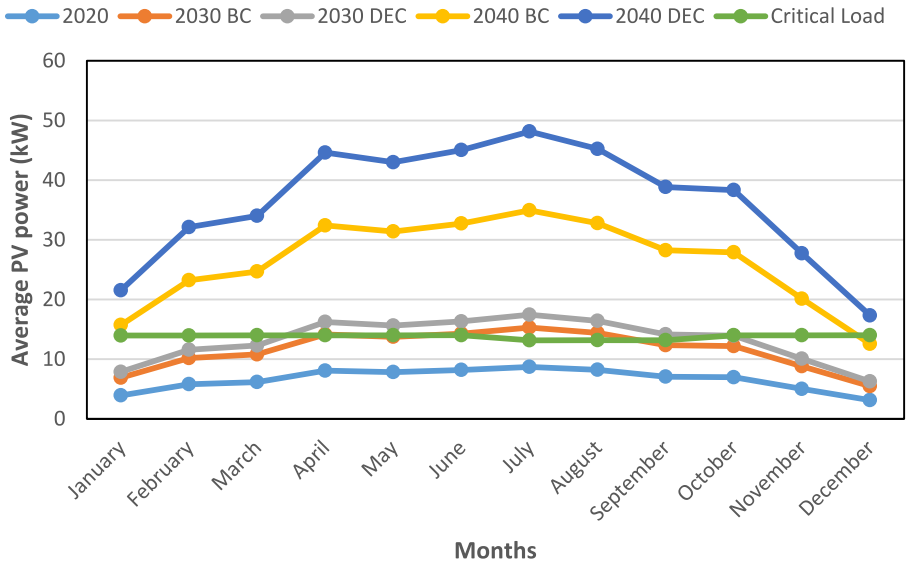

Fig. 7. Average available PV generation and critical load in islanded mode in the car park microgrid.

be seen, as the sizes of the PV generators are significantly higher. Although these plants cannot provide enough energy in October, overall, the scenarios show higher energy availability in island operation than in other scenarios, especially in December. These fluctuations in last three scenarios determinates a drop in the flexible contribution (*FER*), as shown in Table 5.

Considering Table 6, it is worth mentioning that from the 2020 to 2040 DEC scenario, even if the size of PV and wind installations increases, the resilience of the residential microgrid worsens, as indicated by the decrease in the RFR and RDR indices, and the increase in LOLE and ENS indices. Indeed, by increasing consumption and RES capacity by 20 and 62% respectively, the RFR index decreases by 31%. Therefore, the microgrid in islanded mode might be more resilient in the former scenarios than in the latter. Observing Fig. 10, it can be seen that there is a significant difference between the average power output of RES and the critical load in off-grid mode, the consumption decreases in spring, summer and autumn, while the generation of PV and wind systems increases. Therefore, the average ESS energy in different months extracted from the OPF execution could influence the resilience of the microgrid.

Fig. 11 represents this situation. The energy available in the ESS during the islanded operation for the most resilient energy scenarios (2020 and 2030 DEC) has a straight line in a year, while for other scenarios, especially those with more power from renewables, the average energy of ESS is reduced in some months of the year because the optimization of the daily operation causes storage systems to share their energy to reduce the energy purchased from the main grid. Therefore, in these scenarios, the contribution of ESSs in islanded operation decreases (RES factor) and due to the large difference between the critical load and the generation from RES, a large increase in non-supplied energy is expected. Consequently, in the residential area, increased power flow from renewable sources, which is one of the most significant self-healing techniques, does not necessarily lead to increased

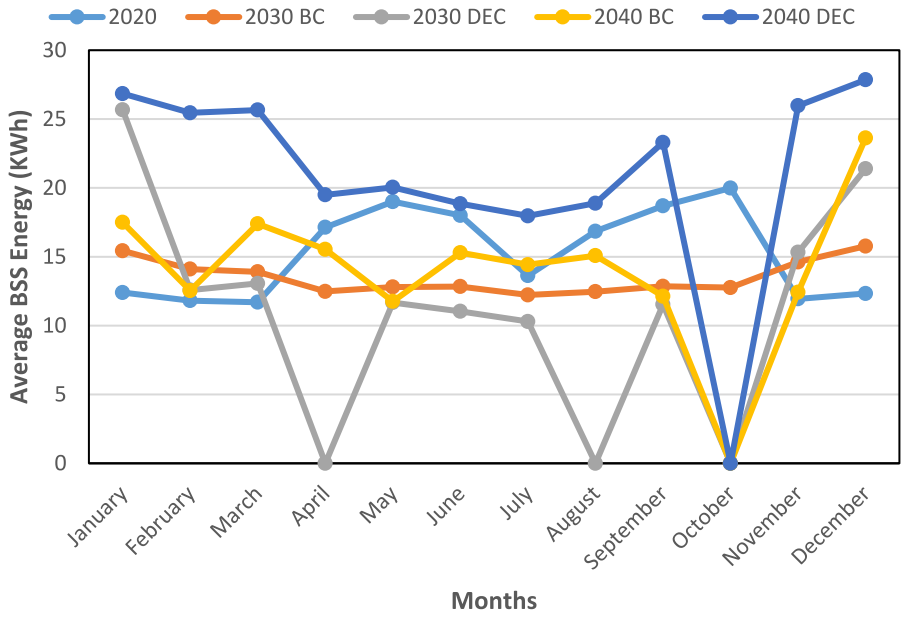

Fig. 8. Average available ESS energy in islanded mode in the car park microgrid.

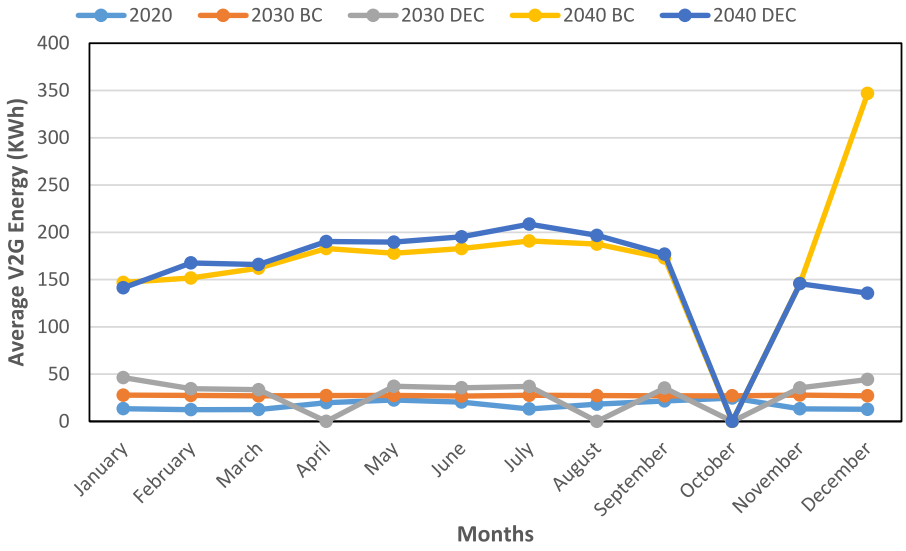

Fig. 9. Average V2G energy available in islanded mode in car park microgrid.

resilience, given the role that OPF plays in the management of the ESSs.

5. Conclusion

A stochastic simulation-based approach has been proposed to evaluate self-healing capacity in hybrid AC/DC microgrids with flexible distributed resources in various energy scenarios. Microgrids operates in islanded mode when a fault occurs in the main AC grid and the goal of the simulations is to determine how likely these microgrids are able to supply their critical loads during island operation, using some self-healing measures such as the implementation of renewable resources, load shedding, and flexible resources (EVs and ESS systems). The performed analysis on three test microgrids shows how the consumption of critical loads in island mode, the installed capacity of RESs, the type of flexible resources, and a suitable OPF may affect self-healing factors. In the underground area, that is the simplest microgrid considered in our study, an increase in PV capacity leads to an increase in resilience; so here it would be said that capacity of RES plays the most significant role. However, in the car park zone, although in the future scenarios there is an higher RESs capacity, OPF sometimes have an adverse impact on self-healing capacity because before the island operation the optimization algorithm decides to discharge V2G smart vehicles and ESS. Residential area shows a completely different behavior comparing to the underground one due to the much more consumption than RESs capacity. In this area, in the scenarios with more RESs capacity, OPF plays a significant role to change the SoC of flexible resources leading to a decrease in these sources in island mode and resilience rates consecutively. Therefore; this paper showed clearly how different parameters and operation control modes might change resilience factors in island mode. For future works, the authors are interested in attacking different control strategies in power sharing among resources and demand response techniques. In addition, it would be worth to consider other AC/DC components like converters in self-healing capability since they can be operate

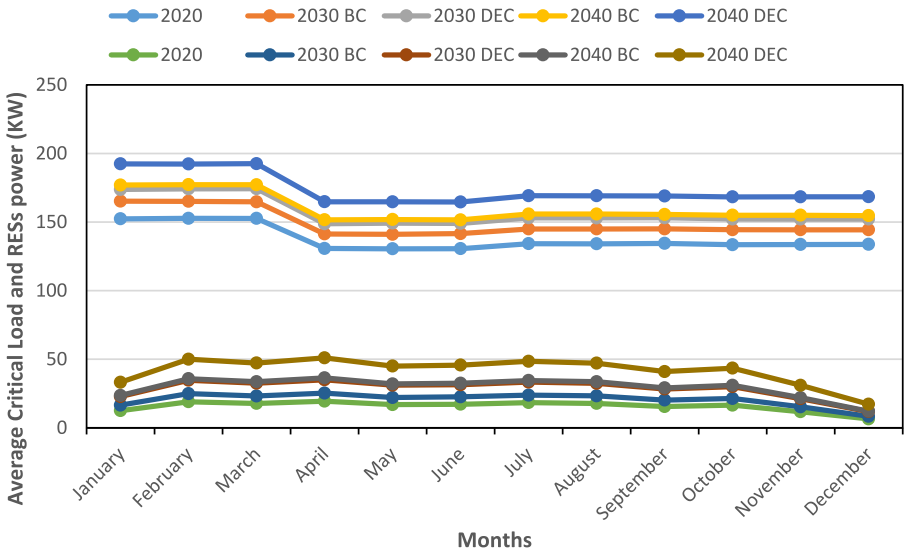

Fig. 10. Average available RESs generation and critical load in islanded mode in residential area.

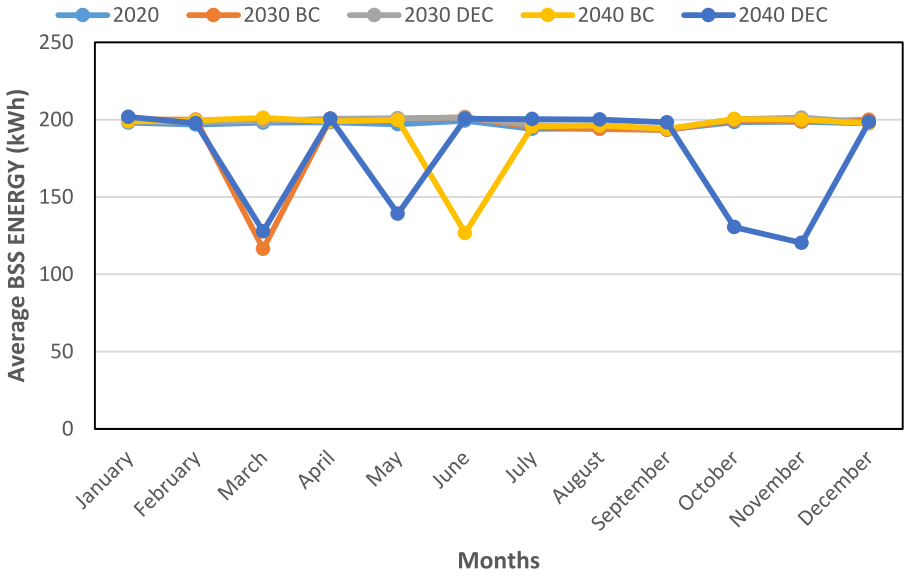

Fig. 11. Average BSS energy available in islanded mode in residential area.

or blocked depending on technical parameters like voltage and frequency.

CRediT authorship contribution statement

Salar Moradi: Conceptualization, Methodology, Software, Formal analysis, Data curation, Writing – original draft, Project administration. **Gaetano Zizzo:** Conceptualization, Methodology, Formal analysis, Resources, Writing – review & editing, Visualization, Supervision, Project administration. **Salvatore Favuzza:** Writing – review & editing. **Fabio Massaro:** Writing – review & editing.

Declaration of competing interest

The authors declare that they have no known competing financial interests or personal relationships that could have appeared to influence the work reported in this paper.

Data availability

Data will be made available on request.

Appendix

Nomenclature

Sets

e	Set of energy scenarios
m	Set of microgrids
t	Set of time intervals a day
s	Set of simulation samples
l	Set of loads
i	Set of island modes
q	Set of time intervals that V2G vehicles are out

Parameters

σ/μ	Normal distribution parameters
β/α	Weibull distribution parameters

$w_i/w_o/w_r$	Cut-in, cut-out and rated wind speed
P_w^r	Rated power of wind turbines
c_g	Electricity price purchased from the main grid
P_{v1}^{ch}	Power consumption by V1G vehicles
η	Efficiency of generation for RESs
P_{pv}^{max}/P_w^{max}	Upper limit for RESs generation
$P_{ch,s}^{max}/P_{ch,s}^{min}$	Upper and lower limits for storage system charge
$P_{dis,s}^{max}/P_{dis,s}^{min}$	Upper and lower limits for storage system discharge
$P_{ch,v2}^{max}/P_{ch,v2}^{min}$	Upper and lower limits for V2G vehicles charge
$P_{dis,v2}^{max}/P_{dis,v2}^{min}$	Upper and lower limits for V2G vehicles discharge
$U_s(0)/U_{v2}(0)$	Initial available energy at ESS and EV park
$\Delta U_s/\Delta U_v$	Small off-set energy to avoid end-of-horizon effect at BES and EV's parking
E_s^{max}/E_s^{min}	Upper and lower limit for energy at ESS
$E_{v2}^{max}/E_{v2}^{min}$	Upper and lower limit for energy at EV park
T_l	Time at which V2G vehicles leave the park
N	Number of V2G vehicles at car park
λ	Discharge rate of EVs
D	Average distance of movement each EV traverses a day
T_r	Number of time intervals microgrid is resilient
T_f	Number of time intervals during a fault (island mode)
P_l^c	Critical load consumption in each microgrids

Variables

$N(.)$	Normal distribution function
$W(.)$	Weibull distribution function
w	Wind speed
P_{pv}/P_w	Power generation of PV and wind system
C_{op}	Total operation cost
P_g	Power purchased from the main grid
P_s^{ch}/P_s^{dis}	Charge and discharge power of ESS
P_{v2}^{ch}/P_{v2}^{dis}	Charge and discharge power of V2G
I_s^{ch}/I_s^{dis}	Binary variable shows charge and discharge status of ESS
I_{v2}^{ch}/I_{v2}^{dis}	Binary variable shows charge and discharge status of V2G vehicles
E_s/E_{v2}	Available energy at ESS and V2G park
P_l	Load of microgrids before fault event
P_{RES}^i	Available power of RESs in island mode
P_F^i	Available power of flexible sources in island mode

References

[1] S. Parhizi, et al., State of the art in research on microgrids: A review, Ieee Access 3 (2015) 890–925.
[2] H. Jiayi, et al., A review on distributed energy resources and MicroGrid, Renew. Sustain. Energy Rev. 12 (9) (2008) 2472–2483.
[3] R.A. Kaushik, N.M. Pindoriya, A hybrid AC-DC microgrid: Opportunities & key issues in implementation, in: 2014 International Conference on Green Computing Communication and Electrical Engineering, ICGCCEE, IEEE, 2014.
[4] JJ. Justo, F. Mwasilu, J. Lee, JW. Jung, AC-microgrids versus DC-microgrids with distributed energy resources: A review, Renew. Sustain. Energy Rev. (2013).
[5] E. Unamuno, J.A. Barrena, Hybrid ac/dc microgrids—Part I: Review and classification of topologies, Renew. Sustain. Energy Rev. 52 (2015) 1251–1259.
[6] E. Unamuno, J.A. Barrena, Hybrid ac/dc microgrids—Part II: Review and classification of control strategies, Renew. Sustain. Energy Rev. 52 (2015) 1123–1134.
[7] Z. Wang, et al., Research on the structures and application scenarios of medium voltage AC-DC hybrid distribution network, in: 2019 IEEE 3rd Information Technology, Networking, Electronic and Automation Control Conference, ITNEC, IEEE, 2019.
[8] M.N. Ambia, H.K. Meng, W. Xiao, Z.Y. Dong, Nested formation approach for networked microgrid self-healing in islanded mode, IEEE Trans. Power Deliv. 36 (1) (2021) 452–463.
[9] Z. Wang, J. Wang, Self-healing resilient distribution systems based on sectionalization into microgrids, IEEE Trans. Power Syst. 30 (6) (2015) 3139–3149.
[10] W. Sun, S. Ma, I. Alvarez-Fernandez, R.R. Nejad, A. Golshani, Optimal self-healing strategy for microgrid islanding, IET Smart Grid 1 (4) (2018) 143–150.
[11] M.A. Owaifeer, M. Al-Muhaini, MILP-based technique for smart self-healing grids, IET Gener. Transm. Distrib. 12 (10) (2018) 2307–2316.
[12] Y. Jia, C.S. Lai, Z. Xu, S. Chai, K.P. Wong, Adaptive partitioning approach to self-sustained smart grid, IET Gener. Transm. Distrib. 11 (2) (2017) 485–494.
[13] S.A. Arefifar, Y.A.-R.I. Mohamed, T.H. EL-Fouly, Comprehensive operational planning framework for self-healing control actions in smart distribution grids, IEEE Trans. Power Syst. 28 (4) (2013) 4192–4200.
[14] A. Golshani, W. Sun, Q. Zhou, Q.P. Zheng, J. Wang, F. Qiu, Coordination of wind farm and pumped-storage hydro for a self-healing power grid, IEEE Trans. Sustain. Energy 9 (4) (2018) 1910–1920.
[15] A. Golshani, W. Sun, K. Sun, Advanced power system partitioning method for fast and reliable restoration: Toward a self-healing power grid, IET Gener. Transm. Distrib. 12 (1) (2018) 42–52.
[16] M. Zadsar, M.R. Haghifam, S.M.M. Larimi, Approach for selfhealing resilient operation of active distribution network with microgrid, IET Gener. Transm. Distrib. 11 (18) (2017) 4633–4643.
[17] A. Elmitwally, M. Elsaid, M. Elgamal, Z. Chen, A fuzzy-multiagent self-healing scheme for a distribution system with distributed generations, IEEE Trans. Power Syst. 30 (5) (2015) 2612–2622.
[18] J.B. Leite, J. Mantovani, Development of a self-healing strategy with multiagent systems for distribution networks, IEEE Trans. Smart Grid 8 (5) (2017) 2198–2206.
[19] Z. Wang, B. Chen, J. Wang, C. Chen, Networked microgrids for selfhealing power systems, IEEE Trans. Smart Grid 7 (1) (2016) 310–319.
[20] Z. Wang, B. Chen, J. Kim, Decentralized energy management system for networked microgrids in grid-connected and islanded modes, IEEE Trans. Smart Grid 7 (2) (2016) 1097–1105.
[21] A. Sujil, R. Kumar, R.C. Bansal, Multi agent based autonomous energy management system with self-healing capabilities for a microgrid, IEEE Trans. Ind. Inform. 15 (12) (2019) 6280–6290.
[22] A. Golshani, W. Sun, Q. Zhou, Q.P. Zheng, J. Tong, Two-stage adaptive restoration decision support system for a self-healing power grid, IEEE Trans. Ind. Inform. 13 (6) (2017) 2802–2812.
[23] H. Lin, et al., Self-healing attack-resilient PMU network for power system operation, IEEE Trans. Smart Grid 9 (3) (2016) 1551–1565.
[24] A. Bonì, S. Favuzza, M.G. Ippolito, F. Massaro, S. Moradi, R. Musca, V. Porgi, G. Zizzo, Analysis of scenarios for assessing the reliability of AC/DC hybrid microgrids – Part I: Underground Station and Car Park, in: IEEE EEEIC/I & CPS Europe 2021, Bari (Italy, 2021.
[25] A. Bonì, S. Favuzza, M.G. Ippolito, F. Massaro, S. Moradi, R. Musca, V. Porgi, G. Zizzo, Analysis of scenarios for assessing the reliability of AC/DC hybrid microgrids – Part II: Residential area and port area, in: IEEE EEEIC/I & CPS Europe 2021, Bari (Italy), 2021.
[26] School of Management - Politecnico Di Milano, Energy & Strategy Group, Renewable Energy Report, Energy Strategy Group & Politecnico di Milano, Milano, 2020.
[27] Eurostat, Energy, transport and environment statistic, 2019.
[28] REN 21, Renewables 2019 Global Status Report, REN 21, 2019.
[29] Terna SpA, SNAM documento di descrizione degli scenari 2019, 2019.
[30] IRENA, Global Energy Transformation, a Roadmap to 2050, IRENA, 2018.
[31] IRENA, Electricity Storage and Renewables: Costs and Markets to 2030, IRENA, 2017.
[32] RSE, Analisi di Impatto Dell'Introduzione Della Tariffa Bioraria Obbligatoria, Technical Report 13000580, 2012.
[33] ARERA, Dati sulla continuità del servizio elettrico, https://www.arera.it/sas-frontend-cse/estrattoreLink.
[34] H. Farzin, M. Fotuhi-Firuzabad, M. Moeini-Aghtaie, Stochastic energy management of microgrids during unscheduled islanding period, IEEE Trans. Ind. Inform. 13 (3) (2017) 1079–1087.
[35] GAMS, Cplex 12, https://www.gams.com/33/docs/S_CPLEX.html.
[36] A.R. Jordehi, How to deal with uncertainties in electric power systems? A review, Renew. Sustain. Energy Rev. (2018).
[37] PNIEC (piano nazionale integrato per l'energia e il clima), 2019, available at: https://www.mise.gov.it/images/stories/documenti/PNIEC_finale_17012020.pdf, accessed 11/02/2022.